Metabolic Engineering 49 (2018) 164–177

Contents lists available at ScienceDirect

Metabolic Engineering

journal homepage: www.elsevier.com/locate/meteng

Systematic overexpression study to find target enzymes enhancing production of terpenes in *Synechocystis* PCC 6803, using isoprene as a model compound

Elias Englund[a,b], Kiyan Shabestary[b], Elton P. Hudson[b], Pia Lindberg[a,*]

[a] Department of Chemistry – Ångström, Uppsala University, Box 523, SE-751 20 Uppsala, Sweden
[b] School of Biotechnology, KTH – Royal Institute of Technology, Science for Life Laboratory, Stockholm, Sweden

ARTICLE INFO

Keywords:
Metabolic engineering
Cyanobacteria
Isoprene
MEP pathway
Metabolic modeling
Carbon flux

ABSTRACT

Of the two natural metabolic pathways for making terpenoids, biotechnological utilization of the mevalonate (MVA) pathway has enabled commercial production of valuable compounds, while the more recently discovered but stoichiometrically more efficient methylerythritol phosphate (MEP) pathway is underdeveloped. We conducted a study on the overexpression of each enzyme in the MEP pathway in the unicellular cyanobacterium *Synechocystis* sp. PCC 6803, to identify potential targets for increasing flux towards terpenoid production, using isoprene as a reporter molecule. Results showed that the enzymes Ipi, Dxs and IspD had the biggest impact on isoprene production. By combining and creating operons out of those genes, isoprene production was increased 2-fold compared to the base strain. A genome-scale model was used to identify targets upstream of the MEP pathway that could redirect flux towards terpenoids. A total of ten reactions from the Calvin-Benson-Bassham cycle, lower glycolysis and co-factor synthesis pathways were probed for their effect on isoprene synthesis by co-expressing them with the MEP enzymes, resulting in a 60% increase in production from the best strain. Lastly, we studied two isoprene synthases with the highest reported catalytic rates. Only by expressing them together with Dxs and Ipi could we get stable strains that produced 2.8 mg/g isoprene per dry cell weight, a 40-fold improvement compared to the initial strain.

1. Introduction

Cyanobacteria, the only bacteria capable of oxygenic photosynthesis, offer a truly sustainable production platform for making valuable compounds directly from light, CO_2 and water. Due to their simple growth requirements, they can be an attractive host for large scale production of biofuel and commodity chemicals, but also for molecules of higher value. Terpenoids are a large and diverse group of natural products composed of many interesting targets for microbial production. Photosynthetic production of terpenoids that could be used as fuels or chemical feed-stocks such as isoprene (Lindberg et al., 2010), squalene (Choi et al., 2016; Englund et al., 2014), β-phellandrene (Bentley et al., 2013) and bisabolene (Davies et al., 2014) have all been successfully demonstrated in cyanobacteria, but also more complex, high-value terpenoids such as the precursors to the medical compounds forskolin (Englund et al., 2015) and artemisinin (Choi et al., 2016).

All terpenoids are synthesized from the same two five-carbon precursor molecules isopentenyl diphosphate (IPP) and dimethylallyl diphosphate (DMAPP) (Fig. 1). IPP and DMAPP are in turn made through the methylerythritol-4-phosphate (MEP) pathway in most bacteria and in the chloroplasts of plants and algae, or through the mevalonate (MVA) pathway in eukaryotic organisms and archaea, as well as in some bacteria (Chang et al., 2013). Production of terpenoids in heterotrophic bacteria such as *Escherichia coli* (*E. coli*) have generally seen higher success using an introduced MVA pathway than with the native, more recently discovered MEP pathway (Eisenreich et al., 2004; Leavell et al., 2016), due to a largely unknown regulation of the MEP pathway (Martin et al., 2003), and the difficulty in balancing the enzymes of the pathway (Ajikumar et al., 2010). In cyanobacteria however, introducing the heterologous MVA pathway to increase terpenoid production have yielded more modest results. In one study, expression of the seven enzymes needed to complete the MVA pathway in *Synechocystis* sp. PCC 6803 (from here on referred to as *Synechocystis*) led to an increase in isoprene titers by 2.5 times (Bentley et al., 2014), compared to 800 times increase in isoprene when the same group expressed the pathway in *E. coli* (Zurbriggen et al., 2012). Also, the use of

* Corresponding author.
E-mail address: pia.lindberg@kemi.uu.se (P. Lindberg).

https://doi.org/10.1016/j.ymben.2018.07.004
Received 6 April 2018; Received in revised form 28 June 2018; Accepted 8 July 2018
Available online 17 July 2018

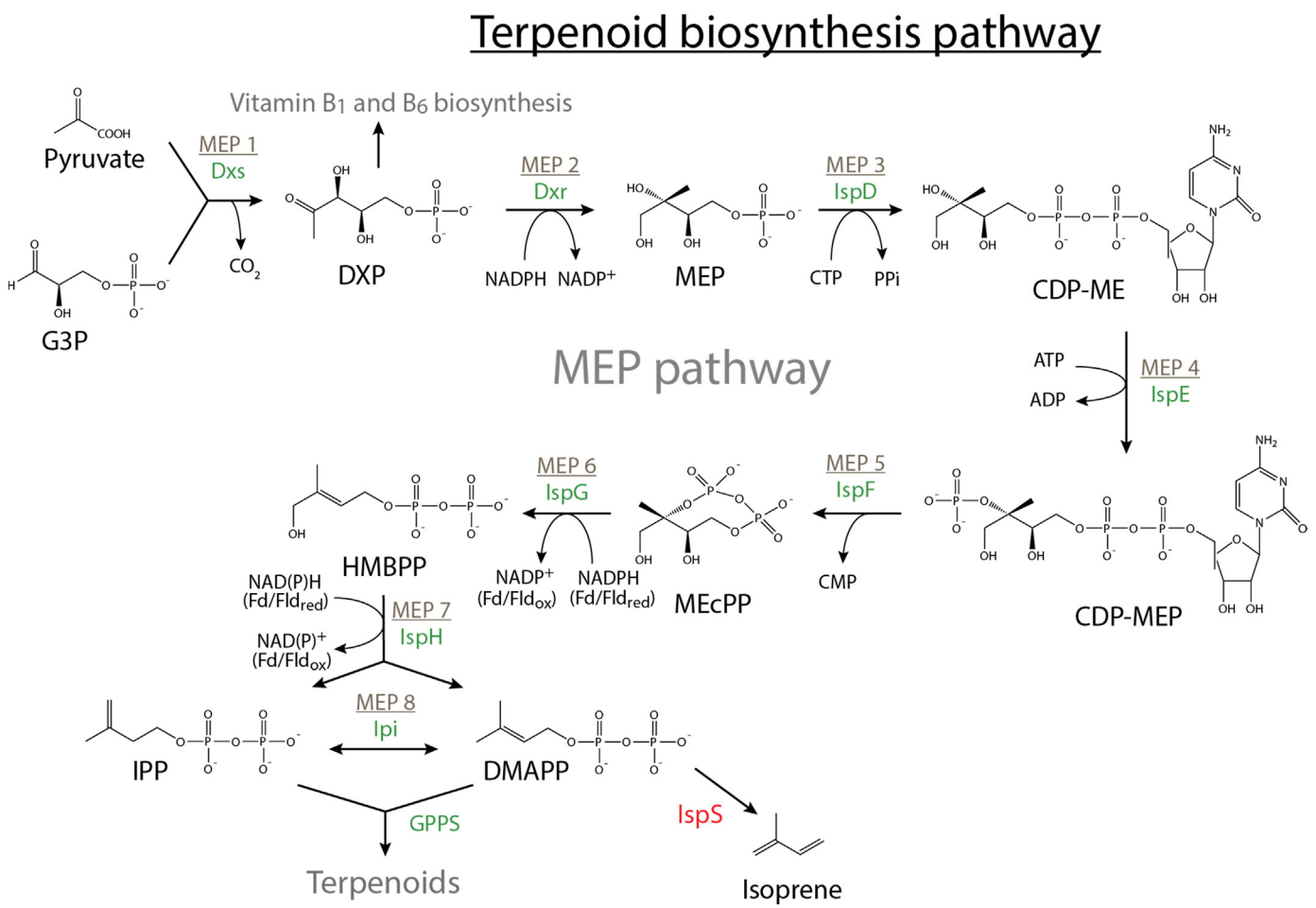

Fig. 1. The MEP biosynthesis pathway of terpenoids with isoprene reaction. Abbreviations used: G3P = glyceraldehyde 3-phosphate, DXP = 1-deoxy-D-xylulose 5-phosphate, MEP = 2-C-methyl-D-erythritol 4-phosphate, CDP-ME = 4-diphosphocytidyl-2-C-methyl-D-erythritol, CDP-MEP = 4-diphosphocytidyl-2-C-methyl-D-erythritol 2-phosphate, ME-cPP = 2-C-methyl-D-erythritol 2,4-cyclodiphosphate, HMBPP = 4-hydroxyl-3-methylbut-2-enyldiphosphate, IPP = isopentenyl diphosphate, DMAPP = dimethylallyl diphosphate, Dxs = DXP synthase, Dxr = DXP reductoisomerase, IspD = MEP cytidylyltransferase, IspE = CDP-ME kinase, IspF = ME-cDP synthase, IspG = HMBDP synthase, IspH = HMBDP reductase, Ipi = IPP isomerase, GPPS = geranyl diphosphate synthase, IspS = isoprene synthase, NADP(H) = nicotinamide adenine dinucleotide phosphate, CTP/CMP = cytidine tri(mono)phosphate, PPi = diphosphate, ATP/ADP = adenosine tri(di)phosphate, $Fd/Fld_{red/ox}$ = ferredoxin/flavodoxin reduced /oxidized.

the MEP pathway has been proposed to be more favorable due to its more efficient use of carbon, with almost 50% higher carbon stoichiometric yield than the MVA pathway (Gruchattka et al., 2013). Utilizing a more carbon efficient pathway is especially important in autotrophically growing cyanobacteria due to the energy investment required for every carbon molecule fixed.

Although the terpenoid synthase can be a limiting step due to their poor catalytic activities (Formighieri and Melis, 2015; Ye et al., 2016), overexpression of key upstream enzymes are usually required to get higher levels of terpenoid product accumulation. Two enzymes in the MEP pathway which have previously been overexpressed in cyanobacteria to increase flux towards terpenoid products are Dxs and Ipi. Although overexpression of Dxs in some cases has resulted in a small (less than 50%) or no increase in flux through the pathway (Gao et al., 2016; Kiyota et al., 2014; Pade et al., 2016), we were in an earlier study able to achieve up to a 4.2 times increase, possibly due to the choice of expressing a non-native plant Dxs, which could be less susceptible to native regulation (Englund et al., 2015). Ipi maintains the balance between IPP and DMAPP, which can be altered in heterologous terpenoid producing strains. In all reports we have found in the literature, expressing Ipi positively affected terpenoid titers (Choi et al., 2016; Gao et al., 2016), with the highest increase reported to be 3.5 times more isoprene produced from a strain of *Synechocystis* (Chaves et al., 2016). Although Dxr is a rate limiting enzyme in *E. coli* (Albrecht et al., 1999), in *Synechococcus elongatus* PCC 7942, it negatively affected amorpha-4,11-diene production, even when co-overexpressed with other MEP enzymes and potentially shifting the bottleneck inside the MEP pathway (Choi et al., 2016). In an isoprene producing *S. elongatus* strain overexpressing both Dxs and Ipi, the MEP intermediate methylerythritol 2,4-cyclodiphosphate (MEcPP) could be seen accumulating. Upon overexpression of IspG, isoprene production increased 1.6 times (Gao et al., 2016).

In addition to bottlenecks within the MEP pathway, reactions in the rest of the metabolism can limit terpenoid production. Due to the complex nature of the complete metabolism, efforts to identify overexpression targets there are lagging behind. Genome-scale models aim to capture such complexity and can be used to drive metabolic engineering beyond the pathway level. Flux balance analysis (FBA) or flux variability analysis (FVA) can be used to solve the system using an objective function (typically biomass) and give a flux distribution value or flux variability, respectively. Different algorithms employing this methodology have been used to identify potential targets for overexpression or down-regulation. Flux scanning based on enforced objective flux (FSEOF; (Choi et al., 2010)) is an FBA-based method whereas flux variability scanning based on enforced objective flux (FVSEOF; (Park et al., 2012)) and OptForce (Ranganathan et al., 2010)

are FVA-based methods. FSEOF and minimization of metabolic adjustment (MOMA) were previously employed to find overexpression and knockout targets, respectively, to improve lycopene titers in *E. coli* (Choi et al., 2010).

When engineering production capabilities such as terpenoid biosynthesis into microorganisms, often times several genes need to be introduced and functionally expressed. However, combinations of promoters, RBSs and coding sequences can lead to unpredictable levels of expression, with one RBS functioning well in combination with one coding sequence but not with another (Kosuri et al., 2013). The cause of this can in part be explained by the 5′UTR formed from the promoter and RBS (Mutalik et al., 2013b), which may create secondary structures preventing efficient translation initiation by the ribosome (Salis et al., 2009). To mitigate this problem, efforts have been made in finding ways of decoupling the expressed gene from its surrounding genetic context, thereby making overexpression more reliable. We have employed two of these so called “genetic insulators” in this study, “bicistronic design” (BCD) and RiboJ. A BCD has a short open reading frame (ORF) placed directly upstream and partially overlapping with the gene of interest (Mutalik et al., 2013a). When the ribosome translates the first coding sequence, it melts secondary structures preventing translational initiation of the downstream gene. Another way is by using enzymatic processing of mRNA, cleaving off the 5′UTR to enable predictable and reliable expression (Qi et al., 2012). RiboJ is such a self-cleaving ribozyme that cuts its own sequence and leaves a 23 nucleotide hairpin structure with an RBS exposed for the ribosome to bind (Lou et al., 2012).

In this work, we created an overexpression assay to test foreign and native enzymes’ capacity to increase flux towards terpenoid synthesis. We started work in *E. coli* to validate the assay and then moved it to *Synechocystis*. Expression was systematically tested with and without genetic insulators to optimize expression for each gene. All MEP enzymes as well as some enzymes from the general metabolism, identified using the FVSEOF methodology, were tested in a standardized way for their ability to enhance isoprene production. Using this method, we discover both novel overexpression targets and reaffirmed known ones.

2. Materials and methods

2.1. Plasmid construction

The sequence for the isoprene synthase from *Pueraria montana* without its chloroplast transit peptide (Lindberg et al., 2010), was codon optimized using the Gene Designer (DNA2.0) software, and synthesized by Biomatik. The gene was inserted into a pET28a vector (Novagen) with a modified multiple cloning site, creating pET PmIspS. All pEEC plasmids were based on the RSF1010 plasmid pPMQAK1 (Huang et al., 2010), modified by replacing the ampicillin and kanamycin cassette with a chloramphenicol cassette. Cloning of gene sequences was done using XbaI and BglII restriction sites on pEEC1, 5 and 7 and BamHI and XbaI sites for pEEC2–4 and 6. The inserted sequences were cut with either XbaI and BamHI (pEEC1, 5, 7) or BglII and XbaI (pEEC2–4, 6) respectively, thereby creating a GGATCT scar from the BamHI and BglII ligation, which is a linker compatible sequence (Anderson et al., 2010). The linker sequence coupled a protein tag already present on the plasmid to the inserted gene, with the exception for cloning into pEEC 5 and 7 where a C-terminal FLAG-tag was included on the amplifying primers. Annotated sequence files of all base pEEC plasmids are available in the Supplementary files. See Fig. 2 and Table 1 for a schematic representation and brief description of base plasmids.

The eight MEP genes and eleven upstream genes or operons were amplified from *E. coli* or *Synechocystis* genomic DNA using primers flanked by the appropriate restriction enzyme sites. If the genetic sequence contained any of the restriction enzyme sites used for cloning, they were removed using overlap extension PCR. Operons were created of PetF FNR, CMPk CDPk Ppa and CTPs Ppa, also by overlap extension PCR. The gene sequences of BbDxs, AtDxs, DrDxs, IbIspS and EgIspS were codon optimized using Gene Designer and synthesized by General Biosystems, while the sequence of CfDxs was amplified from our previously published plasmid (Englund et al., 2015). Plastid transit peptides from eukaryotic genes were removed in accordance to their original studies, the first 40 amino acids from CfDxs (Englund et al., 2015), first 57 amino acids from BbDxs (Matsushima et al., 2012), first 35 amino acids from EgIspS (Gao et al., 2016) and first 49 amino acids from IpIspS (Ilmén et al., 2015). After amplification of genes or operons, they were ligated into their respective pEEC plasmid and sequence verified. For a complete list of gene IDs, see Supplementary Table 1, and for the DNA sequences used, see supplementary sequence files.

2.2. Strains and growth conditions

Escherichia coli strain DH5αZ1 (Expressys) was used for subcloning and BL21 (DE3) (NEB) was used for isoprene and protein measurements. Cultivation was done at 37 °C, except when otherwise noted, in liquid LB medium supplemented with 50 μg ml^{-1} kanamycin for strains carrying a pET vector and/or 35 μg ml^{-1} chloramphenicol for strains with the pEEC vectors. pEEC vectors were transferred into the *SkIspS* strain (Bentley and Melis, 2012), except for p6 IbIspS and p6 EgIspS which were transferred into wild-type *Synechocystis* sp. PCC 6803 by three-parental mating, using the pRL443 conjugative plasmid as described previously (Elhai and Wolk, 1988). *Synechocystis* strains were maintained in 6-well plates at 20 μmol photons m^{-2} s^{-1} and 30 °C in BG11 medium, supplemented with 25 μg ml^{-1} neomycin and/or 20 μg ml^{-1} chloramphenicol.

2.3. Isoprene measurement

E. coli BL21 (DE3) containing pET PmIspS was made competent and transformed with a pEEC vector. Three colonies from LB transformant plates were picked and grown overnight at 25 °C in 24-well plates with LB medium and appropriate antibiotics. Cells were then diluted 100 times, and grown overnight in the same way as the previous day, except with 10 μM IPTG (Sigma-Aldrich) supplemented to the LB. The next day, 100 μl of overnight cultures were seeded into 4.9 ml LB with 10 μM IPTG and antibiotics in 8 ml screw cap tubes (Chromacol 10-SV, ThermoFisher Scientific). After growing the cultures for 24 h at 25 °C, 100 μl of the head space gas was injected in a Clarus 580 Perkin Elmer FID gas chromatograph (GC) with a packed column 353 (1.8 m × 2 mm i.d., Cat No. N9305013-ZW5531, Perkin Elmer). Injection was done through a packed injector, the oven temperature 200 °C for 2.5 min, and the carrier gas was N_2 at 20 ml min^{-1}. The isoprene peak at 1.74 min was compared with a standard curve made using an isoprene standard (Sigma-Aldrich) to convert the area to a mass value. After measuring isoprene, OD_{595} was measured with a Plate Chameleon V Microplate Reader 333 (Hidex), and protein samples were taken and frozen at −80 °C. Every experiment was repeated at least twice, with three biological replicates each time.

For isoprene measurements in *Synechocystis*, cultures growing in 6-well plates at 20 μmol photons m^{-2} s^{-1} were seeded to OD_{750} 0.05–0.1 into 25 ml BG11 with appropriate antibiotics in 100 ml Erlenmeyer-flasks and grown for two days at 50 μmol photons m^{-2} s^{-1}. Then, 15 ml of cultures were pelleted, resuspended in 4 ml BG11 with 50 mM $NaHCO_3$ (Sigma-Aldrich) and 25 mM HEPES (Sigma-Aldrich), transferred to 8 ml screw cap tubes, and grown for an additional 24 h at 50 μmol photons m^{-2} s^{-1}. Isoprene from the head space was then measured in the same way as for *E. coli*, but 150 μl was injected into the GC and a different standard curve was used to convert the peak to a mass value. After measurements were done, OD_{750} was measured the same way as for *E. coli* but with a filter for absorbance at 750 nm, and protein samples were taken and frozen at −80 °C. All strains were grown in

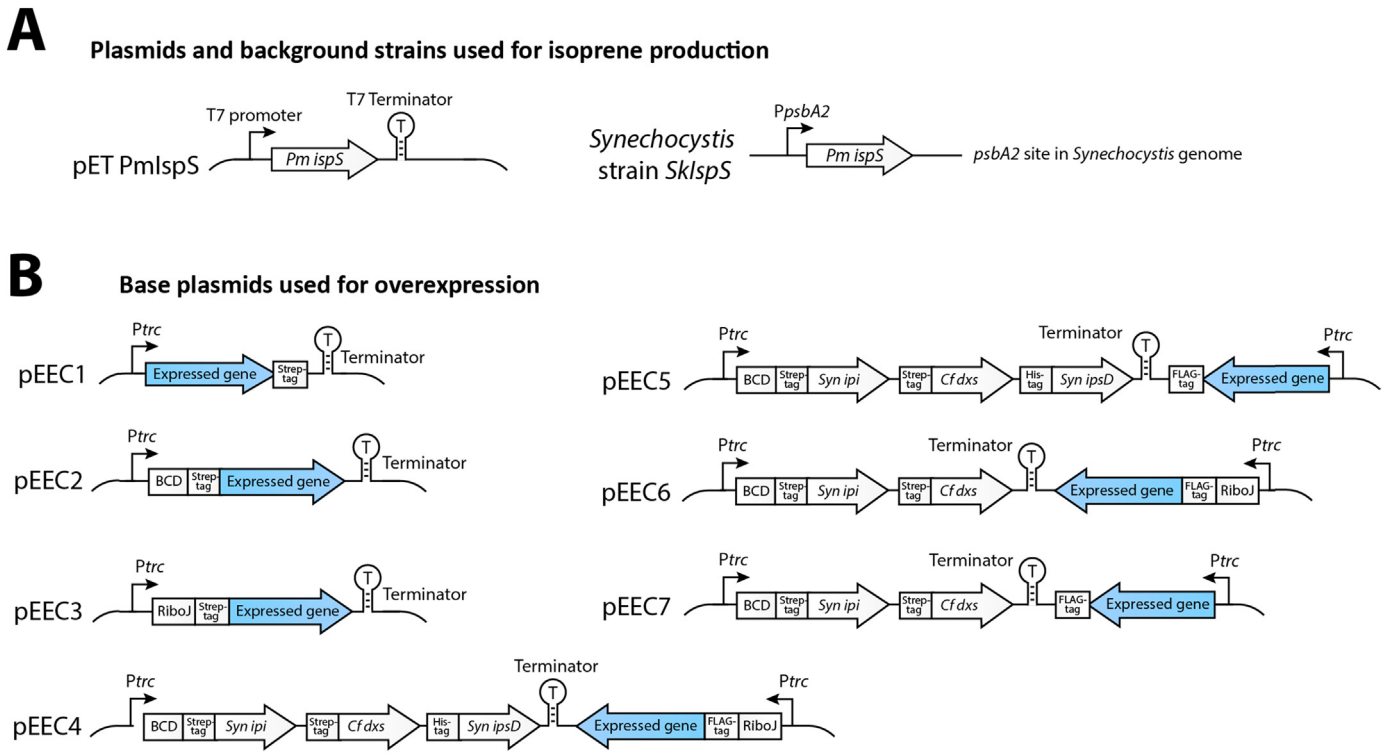

Fig. 2. Schematic overview of plasmids and strains used in this work. (A) Plasmid and strain that was used for isoprene production in *E. coli* and *Synechocystis* (Bentley and Melis, 2012) respectively. (B) Base plasmids used in this study. The blue "Expressed gene" arrow is where a gene or genes in an operon were inserted. (For interpretation of the references to color in this figure legend, the reader is referred to the web version of this article.)

triplicates and each experiment was repeated at least twice. When the overpressure produced in the screw cap tubes caused a leakage, those samples were excluded. Strains referred in the text as being significantly different from the reference strain were compared using the Student's two-tailed *t*-test, $p < 0.05$.

2.4. Protein detection

Frozen *E. coli* pellets were resuspended in water, mixed with 2 × Laemmli Sample Buffer (BIO-RAD) and boiled at 100 °C. The equivalent of 2.8 mg *E. coli* dry cell weight was loaded and separated by sodium dodecyl sulfate polyacrylamide gel electrophoresis (SDS-PAGE). Proteins were then blotted to a membrane using PVDF mini transfer packs (BIO-RAD) and identified using anti-Strep-tactin antibodies (IBA, 2-1502-001, HRP conjugated) and anti-AtpB antibodies (Agrisera, AS05 085). Bands were detected by incubating the membranes with HRP substrate (BIO-RAD). For protein measurements in *Synechocystis*, crude proteins were extracted as described previously (Ivleva and Golden, 2007), and protein concentrations were measured using the DC protein assay (BIO-RAD). Amount loaded ranged from 5 µg to 30 µg, depending on the strength of the signal. After separation and blotting, detection of the proteins were done using a different anti-Strep-tag antibody than for *E. coli* (Abcam, ab76949), an anti-His-tag antibody (Genscript, A00186) or an anti-FLAG-tag antibody (Sigma-Aldrich, F3165). The AtpB antibody was used as a loading control for comparing amounts of protein expressed between strains. All Western immunoblots were repeated at least twice with replicates, results show a representative sample.

For the *E. coli* experiment detecting IspS from the insoluble and soluble fraction, frozen pellets from cultures growing with different amounts of IPTG at 25 °C were washed in phosphate-buffered saline (PBS) buffer at pH 7.5 and freeze-thawed at −80 °C and 37 °C. Cells were then broken using a Precellys 24 bead beater (Bertin Technologies) and the soluble fraction was taken from the supernatant after 1 min centrifugation at 18,000*g*. The leftover pellet was resuspended in the same volume of PBS + 1% SDS as had been taken as supernatant and both fractions were separated by SDS-PAGE.

2.5. Genome-scale modeling

We used an updated version (Shabestary and Hudson, 2016) of the iJN678 genome-scale model (Nogales et al., 2012). Flux balance analysis (FBA) and flux variability analysis (FVA) were performed using the COBRA toolbox 2.0 (Schellenberger et al., 2011) on MATLAB (Mathworks). FVA was used to predict flux ranges while maintaining 99% biomass formation. Complete results can be found in Supplementary Table 2.

3. Results

3.1. Cloning and expression of IspS

Although our primary interest was on studying the MEP pathway in *Synechocystis*, we started our work in *E. coli* to develop an assay that would let us easily and in a relatively high throughput, test the effect of overexpression of enzymes on the flux towards terpenoids. We choose to use isoprene as a reporter molecule. Due to its volatile properties, it readily diffuses out of the cells and accumulates in the head space where sampling is easy. The isoprene synthase from *Pueraria montana* was codon optimized for bacterial expression, synthesized, and cloned into a pET vector under the control of the T7 promoter, thereby creating the plasmid pET PmIspS (Fig. 2A). Successful expression of IspS was confirmed on a protein gel, where the protein was accumulated in the soluble fraction (Fig. S1). Already at 10 µM isopropyl β-D-1-thiogalactopyranoside (IPTG), IspS was highly expressed, and since high concentrations of IPTG can negatively affect isoprene production (Lv et al., 2016), we decided to use that concentration for induction in the following experiments in *E. coli*.

Table 1
List of plasmids and strains used in this study. Constructs named p1 are in pEEC1, p2 in pEEC2 and so on.

Construct	Comment		
pET	Based on pET28a (Novagen) with modified a modified multiple cloning site.		
pET PmIspS	pET with IspS from *Pueraria montana.*		
pEEC1	RSF1010-based expression vector with cloning sites flanked by Ptrc and a C-terminal Strep-tag sequence		
pEEC2	Based on pEEC1, with P*trc* BCD, and the Strep-tag sequence in the N-terminus.		
pEEC3	Based on pEEC1, with P*trc* RiboJ, and the Strep-tag sequence in the N-terminus.		
pEEC4	Based on "p2 SynIpi CfDxs SynIspD", with cloning site in the reverse direction driven by Ptrc RiboJ and with a N-terminus FLAG-tag.		
pEEC5	Based on "p2 SynIpi CfDxs SynIspD", with cloning site in the reverse direction driven by Ptrc and with a C-terminus FLAG-tag.		
pEEC6	Based on "p2 SynIpi CfDxs", with cloning site in the reverse direction driven by Ptrc RiboJ and with an N-terminus FLAG-tag.		
pEEC7	Based on "p2 SynIpi CfDxs", with cloning site in the reverse direction driven by Ptrc and with C-terminus FLAG-tag.		
Strain	**Comment**		
SkIspS	IspS from *Pueraria montana* integrated into the *psbA2* site of *Synechocystis*. Made in Bentley and Melis (2012).		
Construct	**Genes expressed**	**Construct**	**Genes expressed**
p1 EcDxs	*dxs*	**p3 SynIspF**	*ispF*
p1 EcDxr	*dxr*	**p3 SynIspG**	*ispG*
p1 EcIspD	*ispD*	**p3 SynIspH**	*ispH*
p1 EcIspE	*ispE*	**p3 SynIpi**	*ipi*
p1 EcIspF	*ispF*	**p2 SynDxs double Strep**	*dxs*
p1 EcIspG	*ispG*	**p2 SynIpi double Strep**	*ipi*
p1 EcIspH	*ispH*	**p1 EcIspH G120D**	*ispH*
p1 EcIpi	*ipi*	**p1 SynIspH G181D**	*ispH*
p2 EcDxs	*dxs*	**p1 EcDxs Y392F**	*dxs*
p2 EcDxr	*dxr*	**p1 BbDxs**	*dxs*
p2 EcIspD	*ispD*	**p1 AtDxs**	*dxs*
p2 EcIspE	*ispE*	**p1 DrDxs**	*dxs*
p2 EcIspF	*ispF*	**p1 CfDxs**	*dxs*
p2 EIspG	*ispG*	**p2 BbDxs**	*dxs*
p2 EIspH	*ispH*	**p2 AtDxs**	*dxs*
p2 EcIpi	*ipi*	**p2 DrDxs**	*dxs*
p3 EcDxs	*dxs*	**p2 CfDxs**	*dxs*
p3 EcDxr	*dxr*	**p2 SynIpi CfDxs**	*ipi dxs*
p3 EcIspD	*ispD*	**p2 CfDxs SynIpi**	*dxs ipi*
p3 EcIspE	*ispE*	**p2 SynIpi CfDxs SynIspD**	*ipi dxs ispD*
p3 EcIspF	*ispF*	**p4 RbcLXS**	*ipi dxs ispD rbcLXS*
p3 EcIspG	*ispG*	**p5 RbcLXS**	*ipi dxs ispD rbcLXS*
p3 EcIspH	*ispH*	**p4 FbpI**	*ipi dxs ispD fbpI*
p3 EcIpi	*ipi*	**p4 FbaA**	*ipi dxs ispD fbaA*
p1 SynDxs	*dxs*	**p5 FbaA**	*ipi dxs ispD fbaA*
p1 SynDxr	*dxr*	**p4 Pgm**	*ipi dxs ispD pgm*
p1 SynIspD	*ispD*	**p4 Eno**	*ipi dxs ispD eno*
p1 SynIspE	*ispE*	**p4 Pk**	*ipi dxs ispD pk*
p1 SynIspF	*ispF*	**p4 PetF**	*ipi dxs ispD petF*
p1 SynIspG	*ispG*	**p5 PetF**	*ipi dxs ispD petF*
p1 SynIspH	*ispH*	**p4 FNR**	*ipi dxs ispD petH*
p1 SynIpi	*ipi*	**p4 PetF FNR**	*ipi dxs ispD petF petH*
p1 SynDxs	*dxs*	**p5 PetF FNR**	*ipi dxs ispD petF petH*
p2 SynDxr	*dxr*	**p4 CMPk CDPk Ppa**	*ipi dxs ispD CMPk CDPk ppa*
p2 SynIspD	*ispD*	**p4 CTPs Ppa**	*ipi dxs ispD CTPs ppa*
p2 SynIspE	*ispE*	**p6 Pgm**	*ipi dxs pgm*
p2 SynIspF	*ispF*	**p6 Eno**	*ipi dxs eno*
p2 SynIspG	*ispG*	**p6 CTPs PPa**	*ipi dxs CTPs PPa*
p2 SynIspH	*ispH*	**p7 FbaA**	*ipi dxs fbaA*
p2 SsynIpi	*ipi*	**p7 PetF**	*ipi dxs petF*
p3 SynDxs	*dxs*	**p7 PetF FNR**	*ipi dxs petF petH*
p3 SynDxr	*dxr*	**p6 IbIspS**	*ipi dxs ispS*
p3 SynIspD	*ispD*	**p6 EgIspS**	*ipi dxs ispS*
p3 SynIspE	*ispE*		

3.2. Construction of MEP pathway gene overexpression plasmids

Next, we created a base plasmid called pEEC1 from which we would overexpress all eight MEP enzymes from *E. coli* and eight from *Synechocystis* (Fig. 2B). pEEC1 contains the broad host replicon RSF1010 which is functional in both *E. coli* and *Synechocystis*, allowing for the same expression plasmid to be tested in both organisms. Expression is driven by P*trc* which gives a strong inducible expression in *E. coli* and strong constitutive expression in *Synechocystis*. All eight MEP pathway genes from *E. coli* and all eight from *Synechocystis* were cloned into pEEC1 using BglBrick based assembly (Anderson et al., 2010), thereby attaching a Strep-tag to the C-terminus of each MEP gene.

After all genes were cloned into the expression vector, initial tests showed that not all constructs produced detectable amounts of proteins, even though the strong *trc* promoter was used. To circumvent the problem of genes not expressing in certain genetic contexts, we designed new plasmids utilizing genetic elements reported to improve translation initiation and make expression more reliable, bi-cistronic design (BCD) (Mutalik et al., 2013a) in plasmid pEEC2 and RiboJ (Lou et al., 2012) in pEEC3 (Fig. 2B). The position of the Strep-tag was at the same time moved to the N-terminus to simplify the cloning process. After pEEC2 and pEEC3 were constructed, all eight *E. coli* and *Synechocystis* MEP genes were cloned into both plasmids, creating 32 new constructs. See Table 1 for a complete list of plasmids created.

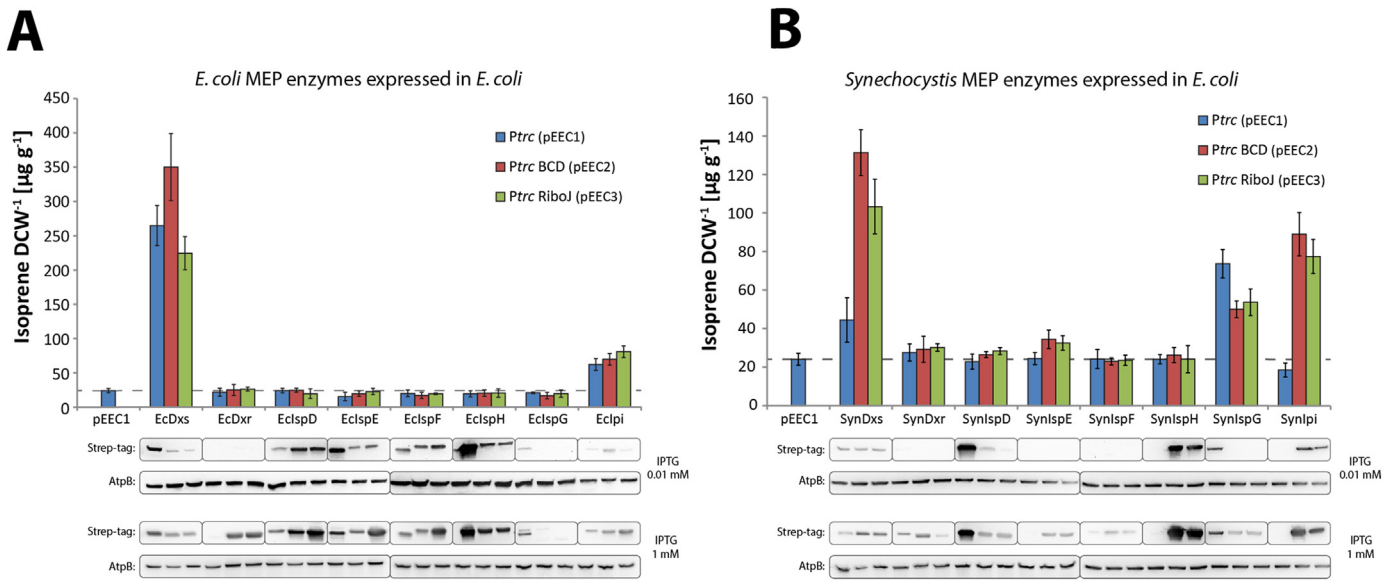

Fig. 3. Isoprene produced and protein accumulation in *E. coli* carrying pET PmIspS and overexpressing one MEP pathway gene from (A) *E. coli* or (B) *Synechocystis*. Blue bars (P*trc*) are genes expressed in pEEC1, red (P*trc* BCD) in pEEC2 and green (P*trc* RiboJ) in pEEC3. The production of reference empty vector strain pEEC1 is marked with a dashed line to better visualize results. All isoprene measurements were done with 0.01 mM IPTG. Proteins were detected on a Western immunoblot with AtpB used as a loading control. Results from isoprene production represent the mean of six biological replicates, error bars represent standard deviation. (For interpretation of the references to color in this figure legend, the reader is referred to the web version of this article.)

3.3. Isoprene production and MEP gene overexpression in E. coli

All MEP expression constructs were transformed into an *E. coli* strain containing pET PmIspS. Isoprene was measured using gas chromatography (GC) and expression levels by Western immunoblot. Although isoprene was measured using 0.01 mM IPTG, we also extracted and detected proteins from cells grown with 1 mM IPTG to get a stronger protein signal and to make it easier to identify differences in overexpression. We observed large variations in protein abundance depending on if the genes were expressed using P*trc*, P*trc* and BCD, or P*trc* and RiboJ. The protein expression pattern from pEEC2 and pEEC3 was highly similar, while it differed in many instances from the pEEC1 based expressions (Fig. 3). Expression of SynIspG with only P*trc* gave higher protein accumulation compared with using BCD or RiboJ, while the pattern was the opposite for SynIspH.

Of the overexpressed *E. coli* MEP genes (denoted Ec"MEP enzyme"), EcDxs, the first enzyme in the pathway, gave by far the highest increase in isoprene production, by 14.5 times when expressed using BCD (Fig. 3A). Expression of the IPP:DMAPP isomerase EcIpi increased isoprene production by 3.4 times, while none of the other *E. coli* enzymes had any effect on isoprene amounts, compared to the empty vector carrying control strain. When expressing the MEP genes from *Synechocystis* (denoted Syn"MEP enzyme"), SynDxs gave a lower isoprene increase than EcDxs did, by 5.4 times while SynIpi had similar activity as EcIpi (Fig. 3B). Also, overexpressing IspG from *Synechocystis* increased isoprene production, something that was not true for EcIspG.

For both SynDxs and SynIpi, expression with BCD or RiboJ gave a much higher effect on isoprene production than expression without. The differences between expression from pEEC1 or from pEEC2 and 3 were not only the use genetic insulators, but also the position of the Strep-tag. If a C-terminal tag affected enzymatic activity for SynDxs and SynIpi, that could explain why expression in pEEC1 was less efficient. However, by putting a tag in both the C- and N-terminus and expressing the two genes with BCD, we could see no decrease in isoprene production, indicating that the tag did not affect the enzymatic activity [Fig. S2].

Other than Dxs and Ipi, the only other enzyme to affect isoprene production was SynIspG, which converts HMBDP to IPP and DMAPP. We reasoned that SynIspG might have a higher DMAPP/IPP production ratio compared to IspG from *E. coli* and that is why EcIspG did not enhance isoprene production. We found in literature a point mutation to *E. coli* IspG that made it selectively produce DMAPP over IPP (Puan et al., 2005). Recreating that mutation did not lead to higher isoprene production in our isoprene assay, nor when mutating the corresponding amino acid in SynIspG (Fig. S2). Further studies on the Michealis Menten parameters of the enzymes would be needed to determine the source of the differences we observe. We also tested a mutation to EcDxs that have been reported to increase activity by several folds (Xiang et al., 2012), but saw no such effect (Fig. S3).

3.4. Assessment of construct functionality in Synechocystis

Next, we wanted to move the MEP overexpression assay into *Synechocystis*. To do so, we first needed to make an isoprene producing background strain. We chose two isoprene synthases that has had high reported activities, *Ipomoea batatas* IspS (IbIspS) (Ilmén et al., 2015) and *Eucalyptus globulus* IspS (EgIspS) (Gao et al., 2016) and attempted to express them in *Synechocystis*. However, we were unable to get a stably expressing strain of either isoprene synthases, possibly due to the effect of the enzymes is detrimental to *Synechocystis*. Instead, we used the strain *SkIspS* that was created and generously provided by the lab of Anastasios Melis (Bentley and Melis, 2012). *SkIspS* has a version of the *P. montana IspS*, codon optimized for expression in *Synechocystis* integrated in the *psbA2* site, where expression is driven by the strong, upstream *psbA2* promoter (Lindberg et al., 2010) (Fig. 2A).

Due to that transferring all 48 constructs used in the *E. coli* study to cyanobacteria would be too time-consuming, we instead decided to select only one construct per gene. To know which of the three constructs to pick for each gene, we first tested if the general expression pattern would be maintained in the new organism, i.e. a strongly expressing construct in *E. coli* would be strongly expressed in *Synechocystis*. The pEEC1 and pEEC2 constructs from the three genes with the highest difference in protein accumulation, SynIspD, SynIspG and SynIpi, were selected and transferred into the *Synechocystis* strain *SkIspS*. When detected on a Western immunoblot with Strep-tag specific antibodies, we could see that the relative protein expression pattern

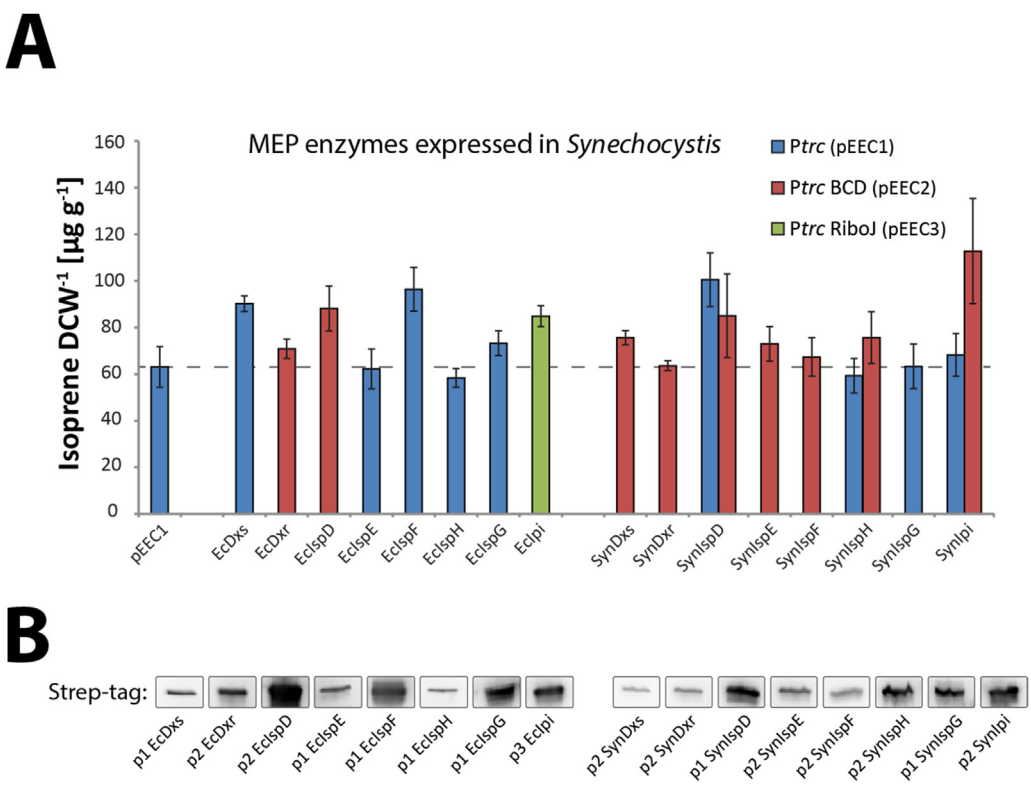

Fig. 4. (A) Isoprene produced in *Synechocystis* strain *SkIspS* overexpressing one MEP pathway gene. Blue bars (P*trc*) are genes expressed in pEEC1, red (P*trc* BCD) in pEEC2 and green (P*trc* RiboJ) in pEEC3. The production of empty vector strain pEEC1 is marked with a dashed line as reference. Results represent the mean of at least three biological replicates, error bars represent standard deviation. (B) Western immunoblot analysis of MEP pathway enzymes. 8 µg of soluble protein fraction were loaded for each strain except for p1 EcIspG where 20 µg was used. (For interpretation of the references to color in this figure legend, the reader is referred to the web version of this article.)

was the same in *Synechocystis* as in *E. coli*, with BCD increasing expression for SynIspG and SynIpi while expression from P*trc* alone resulted in the highest level for SynIspD. This indicates that a strongly expressing construct in *E. coli* has a higher probability to also be strongly expressed in *Synechocystis*. Therefore, we decided to select the highest expressing construct for each MEP gene, based on the *E. coli* data, to transform *Synechocystis* for assessing their effect on terpenoid production.

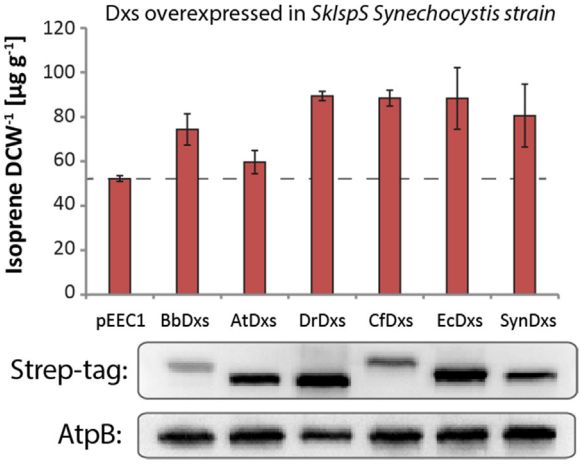

Fig. 5. Heterologous Dxs enzymes expressed in *Synechocystis* strain *SkIspS*. All *dxs* genes were expressed in pEEC2. (Top) Error bars from isoprene measurement represent the standard deviation of at least four biological replicates. The production of empty vector strain pEEC1 is marked with a dashed line to better visualize results the reference sample. BbDxs = *Botryococcus braunii* Dxs, AtDxs = *Agrobacterium tumefaciens* Dxs, DrDxs = *Deinococcus radiodurans* Dxs, CfDxs = *Coleus forskohlii* Dxs, EcDxs = *Escherichia coli* Dxs, SynDxs = *Synechocystis* Dxs. (Bottom) Western immunoblot against Strep-tag attached to the Dxs and AtpB as a loading control. 8 µg of soluble protein fraction was loaded.

3.5. Isoprene production in Synechocystis with overexpressed MEP genes

Constructs overexpressing all eight MEP pathway genes from *E. coli* and *Synechocystis* were conjugated into the *Synechocystis* strain *SkIspS* and isoprene was measured by GC from cultures growing for 24 h in closed tubes. In sharp contrast with the increased production levels reached in *E. coli*, overexpressing EcDxs and SynDxs only improved isoprene production marginally by 1.4 times and 1.3 times (Fig. 4A, see Supplementary Table 3 for absolute amounts). The native SynIpi gave the highest increase with 1.9 times more, while all constructs expressing either isoforms of IspD improved isoprene production. EcIspF gave an increase of 1.5 times, an effect that was not seen when the native enzyme was expressed. After isoprene was measured, cultures were sampled and soluble proteins were extracted and analyzed on a Western immunoblot. Results from the blot clearly demonstrate that all 16 constructs functionally expressed their specific MEP enzymes (Fig. 4B).

3.6. Selecting and expressing heterologous dxs genes

Dxs as the first enzyme in the MEP pathway performs a critical role in bringing flux towards terpenoid biosynthesis, something our *E. coli* assay confirmed. However, the same effect was not observed as strongly in *Synechocystis*. To see if we could find another Dxs that would perform better, we selected an additional four *dxs* genes from different organisms to test. The selection process was based on three criteria: the Dxs enzyme should have (1) a high reported catalytic activity, (2) a high reported increase in product formation when overexpressed or (3) coming from organisms that naturally produce high quantities of terpenoids. From criterion (1), we selected the *dxs* genes from *Agrobacterium tumefaciens* (AtDxs) (Lee et al., 2007) and *Deinococcus radiodurans* (DrDxs) (White et al., 2016), from criterion (2) we selected *dxs* from *Coleus forskohlii* (CfDxs) (Englund et al., 2015) and from (3), *Botryococcus braunii dxs* (BbDxs) (Matsushima et al., 2012). The four *dxs* genes were codon optimized and cloned into pEEC1 (Ptrc) or pEEC2 (Ptrc BCD). To make sure the constructs were working, expression and production was first measured in *E. coli*. All constructs using BCD had a

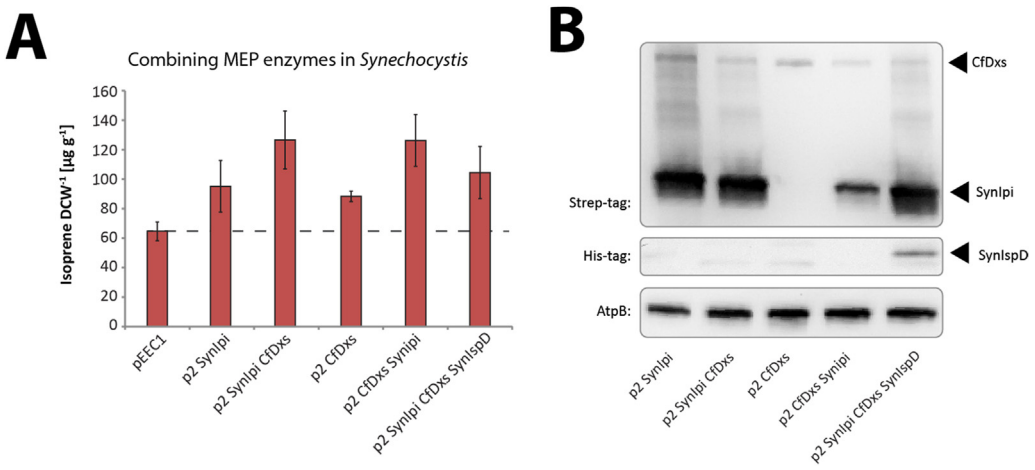

Fig. 6. Combining MEP genes into operons and expressing in *SkIspS* strain. (A) Isoprene production was measured with at least 5 biological replicates, error bars represent standard deviation. The production of empty vector strain pEEC1 is marked with a dashed line to better compare results. (B) Western immunoblot with against Strep-tag (CfDxs and SynIpi), His-tag (SynIspD) or AtpB as loading control. The position and size of proteins are marked with a black arrow. 5 µg of soluble protein fraction were loaded for Strep-tag and AtpB blots, 30 µg for His-tag blot.

stronger expression and/or had a higher increase in isoprene (Fig. S5). Thus, those plasmids for each *dxs* were conjugated into the *Synechocystis SkIspS* strain.

Comparing the effect of the four new *dxs* and previously made EcDxs and SynDxs strains, expression of DrDxs, CfDxs and EcDxs all increased isoprene production the most by 1.7 times (Fig. 5). Dxs has been reported to have solubility problems when expressed in *Synechocystis* (Kudoh et al., 2017). However, we could detect all six isoenzymesin the soluble protein fraction, and all had an effect on increasing the isoprene production indicating that they were active in the cells. Due to CfDxs having among the highest increase in isoprene production even though it was more weakly detected, we concluded that CfDxs was the best performing Dxs per amount of protein in our assay.

3.7. Combing MEP gene expression

In the next step, we combined the best performing MEP genes and expressed them together. The two genes with the highest increase: SynIpi (1.9×) and CfDxs (1.7×) were made into an operon as SynIpi – CfDxs or CfDxs – SynIpi. Co-expressing CfDxs on the p2 SynIpi plasmid increased isoprene production by 1.3× and SynIpi on the p2 CfDxs plasmid by 1.4×, while both gave twice the production compared with the control strain (Fig. 6A). Next, we put the third most efficient MEP gene: SynIspD as the last gene in the SynIpi CfDxs operon. The resulting strain was not enhanced by the presence of SynIspD, but instead made 0.8× the amount of isoprene compared to the SynIpi CfDxs strain, for unknown reasons. The presence of the expressed enzymes could all be detected on a Western immunoblot, although the smear patterns of SynIpi overlapped with the position of CfDxs on the blot, making it hard to separately identifying CfDxs in strains expressing both enzymes (Fig. 6B).

3.8. Modeling of Synechocystis metabolism to find overexpression targets

We next decided to explore the Synechocystis metabolic network beyond MEP enzymes to find non-intuitive overexpression targets for improving isoprene production. Using an updated version of *Synechocystis* genome-scale model (Nogales et al., 2012), we looked at reactions whose flux correlated with flux to isoprene synthesis. This was achieved by iteratively constraining isoprene synthesis to different fluxes and then solving the system with flux variability analysis (FVA). We preferred FVA to FBA because it takes into account reaction variability, making it a more accurate method. We iteratively constrained the flux going to isoprene synthesis to 0, 0.05, 0.1, 0.25 and 0.5 mmol/gCDW/h (67% of the maximal theoretical productivity). In each case, FVA was applied to determine the flux range of each reaction with respect to the isoprene constraint. The most common pattern was a slight reduction (in absolute value) in both upper and lower reaction boundaries, especially for peripheral reactions whose flux scales directly with growth rate. As expected, as flux to isoprene is stepwise increased, less carbon is available for biomass and thus flux ranges of biomass-related reactions decrease. However, for some reactions both lower and upper flux boundaries increased or decreased at levels greater than the biomass related reduction, indicating necessary up- and down-regulations to accommodate higher isoprene flux (see Supplementary Table 2 for FVA results of each reaction). The pathways where reactions were up-regulated were then further investigated for potential overexpression targets.

Overall, our analysis suggests a general up-regulation of the Calvin-Benson-Bassham (CBB) cycle to increase carbon fixation and to generate more of the MEP substrate glyceraldehyde 3-phosphate (G3P, Fig. 7). Since the cycle is fairly complex, with 13 reactions catalyzed by 11 enzymes, we selected three native enzymes that have been shown to increase growth and oxygen evolution when overexpressed: ribulose 1,5-bisphosphate carboxylase/oxygenase (Rubisco, *rbcLXS*) (Liang and Lindblad, 2017), fructose-bisphosphate aldolase class II (*fbaA*) and fructose-1,6-/sedoheptulose-1,7-bisphosphatase (*fbpI*) (Liang and Lindblad, 2016). Although the model did not suggest a clear increase in FbaA reaction flux, we still selected it due to its previously shown effect on increasing carbon fixation.

The model also predicted an up-regulation of the lower part of glycolysis, the catalysis of 3-phosphoglycerate (3PG) in three contiguous steps to pyruvate by phosphoglycerate mutase (Pgm), enolase (Eno) and pyruvate kinase (Pk). Although there are several isoenzymes annotated in *Synechocystis* for the catalytic steps of the lower glycolysis, we selected one enzyme from each reaction.

The model also predicted that the supply of the IspD co-factor cytidine triphosphate (CTP) might become limiting when enough carbon flux is going towards isoprene. Two gene groups were selected to test CTP regeneration. Cytidine monophosphate kinase (CMPk) and cytidine diphosphate kinase (CDPk) which makes CTP, the other nucleoside triphosphates (NTPs) and deoxy-NTPs from ATP, and a CTP synthase (CTPs) that interconverts UTP/CTP. Together with either gene groups, we also expressed the diphosphate to monophosphate converter diphosphatase (Ppa) that was up-regulated in the model due to the release of diphosphate by IspD.

The MEP pathway requires NADPH or reduced ferredoxins in three catalytic steps, the first (Dxs), sixth (IspG) and seventh (IspH). The model had an increased NADPH/ATP ratio requirement that it solved by up-regulating the ferredoxin-$NADP^+$ reductase (FNR), provider of NADPH from light, whereas ATP synthesis was called for down-regulation. Therefore, we selected FNR (*petH*) as a target for overexpression with the aim of increased NAPDH production. Also, it has

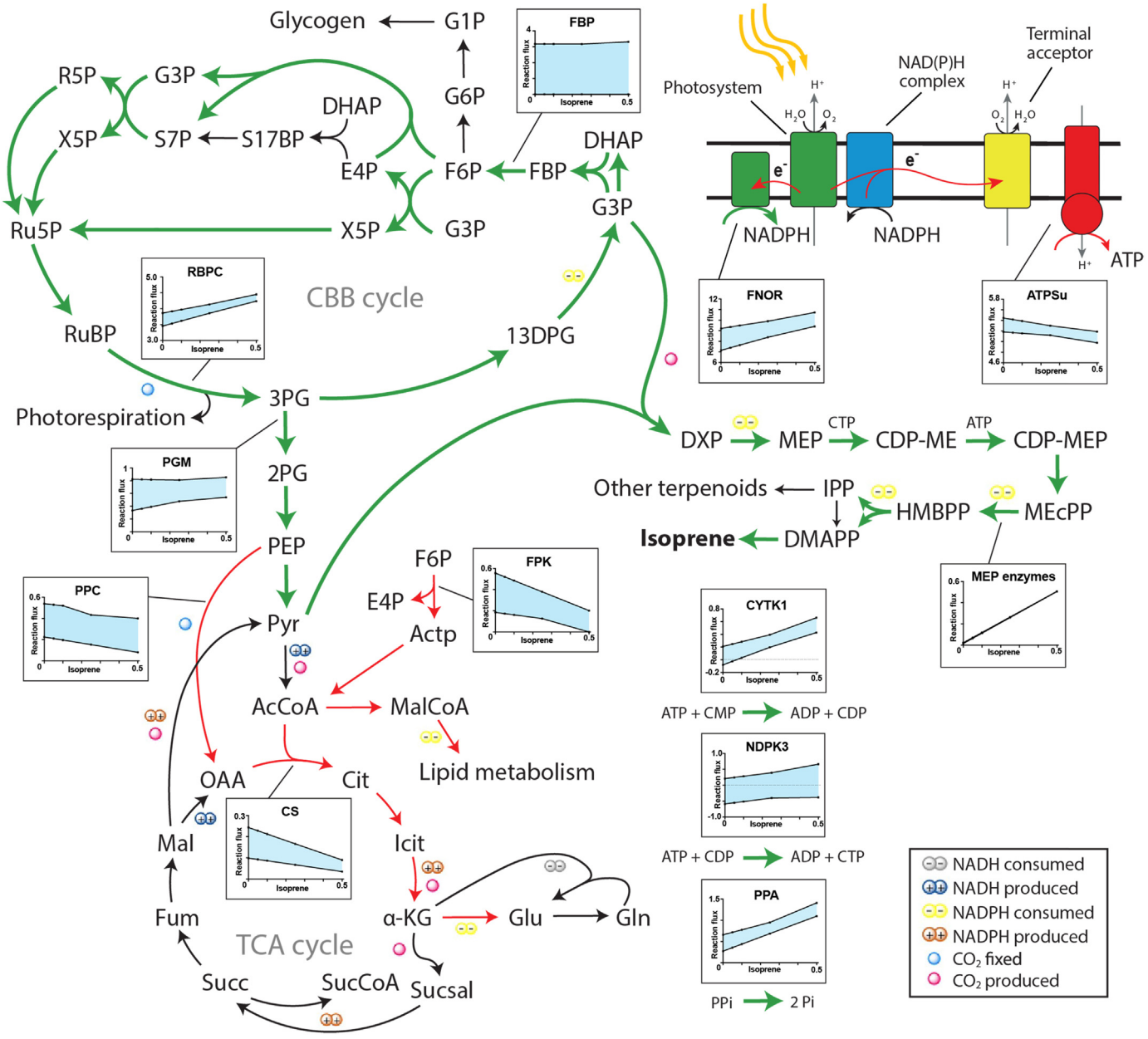

Fig. 7. Overview of flux changes in the metabolism supporting increased isoprene production. Green and red arrows indicate increased and decreased flux reaction respectively. Flux units are in mmol/gDCW/h. 13DPG = 3-phospho-D-glyceroyl phosphate, 2PG = 2-phosphoglycerate, 3PG = 3-phosphoglycerate, α-KG = 2-oxoglutarate, AcCoA = acetyl-CoA, Actp = acetyl phosphate, ATPSu = ATP synthase (thylakoid); CDP-ME = 4-(cytidine 5′-diphospho)-2-C-methyl-D-erythritol, CDP-MEP = 2-phospho-4-(cytidine 5′-diphospho)-2-C-methyl-D-erythritol, Cit = citrate; CS = citrate synthase, CYTK1 = cytidylate kinase (CMPk); DHAP = dihydroxyacetone phosphate, DMAPP = dimethylallyl diphosphate, DXP = 1-deoxy-D-xylulose 5-phosphate, E4P = erythrose 4-phosphate, F6P = fructose 6-phosphate, FBP = fructose-biphosphatase, FDP = fructose 1,6-biphosphate, FNOR = ferredoxin-NADP + reductase (FNR), FPK = fructose phosphoketolase, Fum = fumarate, G1P = glucose 1-phosphate, G3P = glyceraldehyde 3-phosphate, G6P = glucose 6-phosphate, Glu = glutamate, Gln = glutamine, HMBPP = 1-hydroxy-2-methyl-2-(E)-butenyl 4-diphosphate, Icit = isocitrate, IPP = isopentenyl diphosphate, Mal = malonate, MEcPP = 2-C-methyl-D-erythritol 2,4-cyclodiphosphate, MEP = 2-C-methyl-D-erythritol 4-phosphate, NDPK3 = nucleoside-diphosphate kinase (CDPk), OAA = oxaloacetate, PEP = phosphoenolpyruvate, PGM = phosphoglycerate mutase, PPA = inorganic diphosphatase, PPC = phosphoenolpyruvate carboxylase, PPi = diphosphate, Pyr = pyruvate, RBPC = ribulose-biphosphate kinase, R5P = ribose 5-phosphate, Ru5P = ribulose 5-phosphate, RuBP = ribulose 1,5-biphosphate, S17BP = sedoheptulose 1,7-bisphosphate, S7P = sedoheptulose 7-phosphate, Succ = succinate, SucCoA = succinyl-CoA, Sucsal = succinic semialdehyde, X5P = xylulose 5-phosphate. Enzyme abbreviations are the ones used in the model, there are some discrepancies with the abbreviations used in the rest of this article. (For interpretation of the references to color in this figure legend, the reader is referred to the web version of this article.)

previously been shown that the fifth intermediate of the MEP pathway and the substrate of IspG, 2C-methyl-D-erythritol 2,4-cyclodiphosphate (MEcPP) accumulates in the cell when certain MEP genes are overexpressed (Gao et al., 2016). Increased flux through that step have been achieved in *E. coli* by overexpressing the reductant partner of IspG (Zhou et al., 2017). In *Thermosynechococcus elongatus*, IspG has the ability to get electrons from the ferrodoxin PetF which in turn can get them from FNR (Okada and Hase, 2005). There are four PetFs annotated for *Synechocystis* in KEGG. Of those, the PetF *sll0020* had the highest sequence similarity with the PetF interacting with IspG in *T.*

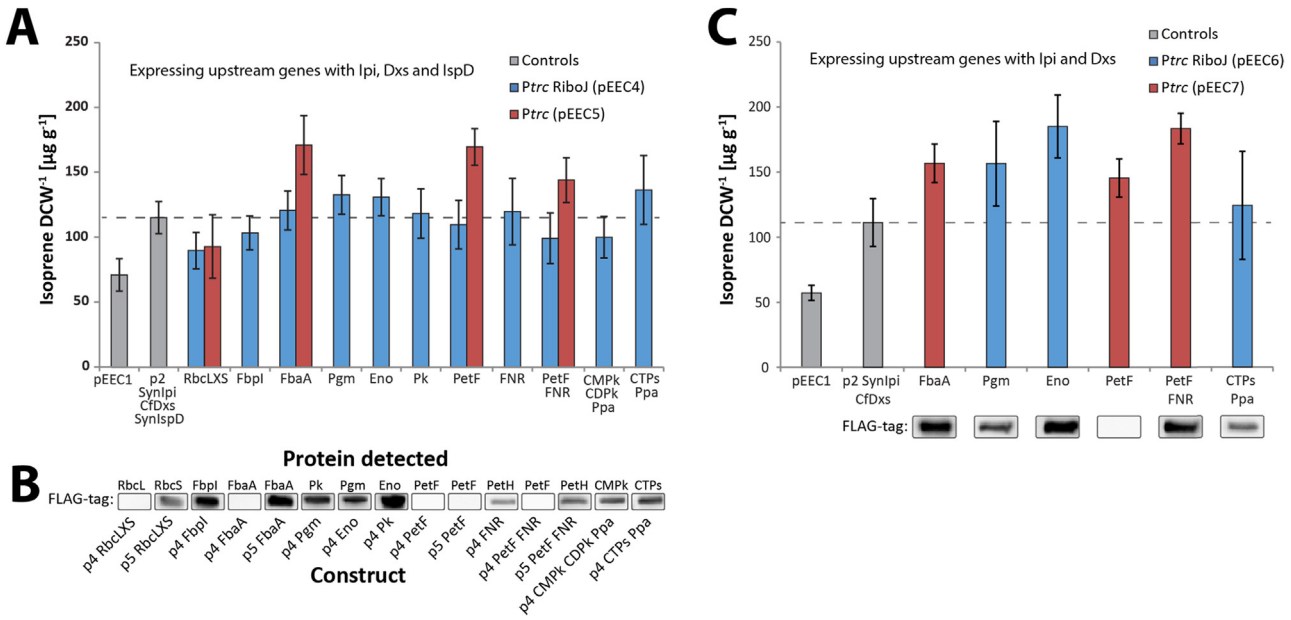

Fig. 8. Effect of upstream targets on isoprene production. (A) Isoprene production when upstream genes were expressed together with SynIpi, CfDxs and SynIspD in pEEC4 (blue bars) or pEEC5 (red bars). Production of reference strain p2 SynIpi CfDxs SynIspD is marked with a dashed line. (B) Western immunoblot against FLAG-tag with 12 µg soluble protein fraction loaded. Due to the N-terminal position of the tag, only the first gene in the operon is detected for pEEC4 (p4) and the last one for pEEC5 (p5) constructs. The actual protein being detected is marked above the blot and which construct being expressed below. (C) Isoprene production when upstream genes were expressed together with SynIpi and CfDxs in pEEC6 (blue bars) or pEEC7 (red bars). Error bars represent the standard deviation of at least five biological replicates. (For interpretation of the references to color in this figure legend, the reader is referred to the web version of this article.)

elongatus. It is also the transcriptionally most abundant of the four and essential for cell viability (Poncelet et al., 1998). Therefore, we choose to overexpress that specific PetF, FNR and both together in an operon to see if that could increase reductant availability for the MEP pathway.

3.9. Testing effect of expression of upstream targets

From the modeling results, eleven genes or genes in operons were selected from *Synechocystis* native metabolism. They were: *rbcLXS* in its native operon, *fbpI*, *fbaA*, *pgm*, *eno*, *pk*, *petF*, *petH* (FNR), *petF petH* in an operon, *CMPk CDPk* and *ppa* in an operon, and *CTPs* and *ppa* in an operon. To test their influence on terpenoid production, a plasmid based on "p2 SynIpi CfDxs SynIspD" was made called pEEC4. The new base plasmid contained an additional expression site driven by the P*trc* promoter with RiboJ and an N-terminal FLAG-tag (Fig. 2). All eleven gene targets were cloned separately into pEEC4 ("p4", see Table 1). After conjugating the plasmids into *SkIspS*, early results indicated that p4 RbcLXS, p4 FbaA, p4 PetF and p4 PetF FNR did not express detectable amounts of the upstream proteins (Fig. 8B). We previously saw that a construct which was poorly expressed by P*trc* RiboJ with an N-terminal tag could get a better expressed with a different 5′UTR sequence (Fig. 3). To achieve that, we modified pEEC4 to instead express the upstream genes using P*trc* and with a C-terminal tag, and then called the new plasmid pEEC5 (Fig. 2). The *fbaA* and *petF* genes along with the *rbcLXS* and *petF petH* operons were cloned into pEEC5 and expressed in the *SkIspS Synechocystis* strain. All new constructs had detectable expression, with the exception of p5 PetF (Fig. 8B).

Production of isoprene was measured for the new strains with "p2 SynIpi CfDxs SynIspD" used as a control. The co-expression of the CBB cycle enzyme FbaA together with SynIpi, CfDxs and SynIspF led to the biggest increase in isoprene production, by 1.5 times (Fig. 8). Over-expressing the two enzymes Pgm and Eno from the lower glycolysis both led to a statistically significant increase by 1.2 and 1.1 times respectively. The ferredoxin PetF also enhanced production, by 1.5 or 1.3 times when in an operon with FNR, while the NADP reductase FNR alone did not. This indicates that although PetF was not detectable on a Western immunoblot, it still had some activity. Lastly, the CTP/UTP interconverter CTP synthase together with Ppa increased production by 1.2 times. From the metabolic model prediction, at least one construct from each selected upstream pathway successfully increased flux towards isoprene, which demonstrates the validity of the method.

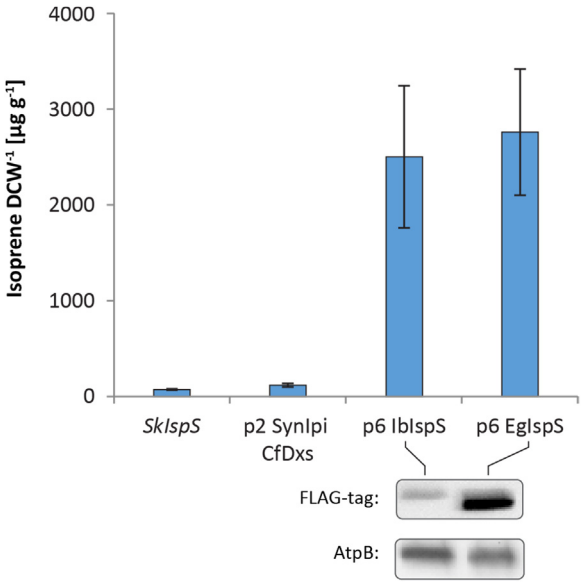

Fig. 9. Isoprene production by *I. batatas* and *E. globulus* IspS expressed together with SynIpi and CfDxs in pEEC6. The IspS was detected with a Western immunoblot against an N-terminal FLAG-tag, AtpB was used as a loading control. 20 µg of soluble protein fraction was loaded for FLAG-tag blot, 8 µg for AtpB blot. Error bars represent the standard deviation of 6 biological replicates.

3.10. Expressing selected upstream targets with SynIpi and CfDxs

In the experiments described above, the upstream genes were

expressed together with SynIpi, CfDxs and SynIspD in pEEC4 or 5. However, comparing "p2 SynIpi CfDxs" with "p2 SynIpi CfDxs SynIspD", the addition of SynIspD actually lowered isoprene production (Fig. 6). Therefore, we made two new base plasmids called pEEC6 and pEEC7, which were identical to pEEC4 and 5 respectively but with SynIspD removed (Fig. 2). All upstream targets that increased production were cloned in the new plasmids (pEEC4 genes into pEEC6, pEEC5 genes into pEEC7) and then transferred into *SkIspS*. When expressed with SynIpi and CfDxs, the enolase Eno increased production the most by 1.7 times compared to p2 SynIpi CfDxs, followed by PetF FNR by 1.6 times and FbaA by 1.4 times (Fig. 8C). Interestingly, when IspD was no longer expressed in the construct, CTP synthase with Ppa no longer increased isoprene flux. The co-factor to IspD is CTP, indicating that it needs to be overexpressed to take advantage of any additional CTP produced.

3.11. Expressing more efficient isoprene synthases

As described earlier, we were initially unable to stably express IbIspS and EgIspS in *Synechocystis*. However, we reasoned that it might be caused by a metabolic imbalance from a too efficient IspS, which could be resolved by co-expressing the isoprene synthases with Dxs and Ipi. Thus, IbIspS and EgIspS were cloned into pEEC6 and conjugated into wild-type *Synechocystis*. The isoprene production from the new isoprene synthases overexpressed with SynIpi and CfDxs was 35 and 39 times higher for IbIspS and EgIspS respectively compared with the *SkIspS* strain expressing the isoprene synthase from *P. montana* and 21 and 24 times higher than the *SkIspS* strain expressing SynIpi and CfDxs (Fig. 9). The p6 EgIspS construct reached production levels of 2.8 mg/g isoprene per dry cell weight. Both IspS were stably maintained in the mutants without noticeable growth defects, indicating that overexpressing Ipi and/or Dxs can counteract the metabolic imbalance that the efficient IspS created.

4. Discussion

With this study, we wanted to find both native and heterologous enzymes that could be expressed in *Synechocystis* to increase terpenoid flux. Relatively few studies have been done on the MEP pathway in cyanobacteria and then, MEP engineering strategies that worked in *E. coli* has typically been used (Halfmann et al., 2014; Kiyota et al., 2014). This study is the first of its kind where the role of every MEP reaction step has been investigated for increased terpenoid production in cyanobacteria in general, and in *Synechocystis* specifically. A series of plasmids were created into which we could amplify and ligate many genes in parallel in a simple cloning step, allowing us to test more genes than is typical in a cyanobacterial study. For each enzyme, expression levels were detected using a protein tag. In cases where the presence of the enzyme was not detected, we change the promoter expression system and moved the tag to the opposite end. This method meant that we could generate at least one construct with expression for each enzyme, with the exception of PetF. It has been reported that a sizeable fraction of many MEP enzymes becomes insoluble when overexpressed in *E. coli* (Zhou et al., 2012) which has also been seen for IspS and Dxs in *Synechocystis* (Kudoh et al., 2017). Even if a portion of the enzymes we overexpressed became insoluble, we could still see a clear accumulation of proteins in the soluble fraction in *Synechocystis* for each gene except one. We also saw that when the same gene was expressed with either BCD or RiboJ, they had similar protein accumulation but different from the pEEC1 constructs without those genetic elements (Fig. 3). A possible explanation would be that BCD and RiboJ share the same function of removing secondary structures blocking translation initiation which could lead to the same expression results (Lou et al., 2012; Mutalik et al., 2013a). Also, constructs with BCD and RiboJ had the same 5′ sequence of the ORF due to both having the peptide tag in the N-terminus, a region that plays a key part in determining expression levels (Kudla et al., 2009).

The results from the MEP overexpression revealed that the biggest impact on isoprene production in *Synechocystis* was from Ipi, Dxs and IspD (Fig. 4), which is in accordance with previous results from cyanobacteria (Gao et al., 2016). Whether Ipi can increase overall flux through the MEP pathway or only affects the IPP/DMAPP partitioning is not known. However, since both IPP and DMAPP acts inhibitory against Dxs (Banerjee et al., 2013) and IspS (Gao et al., 2016), maintaining them in a balance could prevent feedback inhibition on those enzymes. Dxs is frequently described as the "gatekeeper" of the MEP pathway (Davies et al., 2015), controlling influx and by performing a decarboxylation, creates a driving force through the pathway (Shen et al., 2011). This critical role of Dxs for increasing terpenoid flux is not as often seen in cyanobacteria. We could see a sharp contrast between *E. coli* and *Synechocystis* when expressing Dxs, which impacted isoprene production ten-folds more in *E. coli*. The difficulty in making large impact on flux towards terpenoid in cyanobacteria can also be seen in the results from studies transferring the MVA pathway into *Synechocystis* (Bentley et al., 2014), which resulted in orders of magnitude less impact on isoprene production than in *E. coli* (Zurbriggen et al., 2012). The difference could be due to the already large proportion of terpenoids cyanobacteria make (Lindberg et al., 2010), so that an additional redirection of flux has less relative impact. It is also possible that cyanobacteria, which require fast adaptation to changes in light and therefore changes in carotenoid and other terpenoid cellular composition, have a more tightly regulated terpenoid biosynthesis, which is less susceptible to modifications.

When the best performing MEP genes were combined and expressed together, the addition of IspD negatively impacted isoprene production (Fig. 6). While the cause of this is unclear, it might be related to a CTP shortage. Expressing CTPs and Ppa in pEEC4 might have negated the negative impact IspD had on isoprene production (Fig. 8A), since the same increase was not seen in pEEC6 without IspD (Fig. 8C). Additionally, while overexpressing IspH did not itself improve production, expressing its expected ferredoxin partner PetF did. Although PetF could not be detected on a Western immunoblot, the increase in isoprene production indicates that it was present and that it plays a role in terpenoid synthesis, possibly by being a reducer of IspH.

Of the CBB cycle genes, expressing FbaA gave an increase in isoprene while RbcLXS and FbpI did not. Although overexpressing Rubisco have in other studies led to more CO_2 fixed and enhanced product formation (Atsumi et al., 2009; Liang et al., 2018), it has also been shown that *Synechocystis* can down-regulate the native gene copy when an additional copy of RbcLXS is expressed, resulting in unaltered levels of the enzyme (Liang and Lindblad, 2016). This makes overexpressions of Rubisco unpredictable and the ribulose-1,5-bisphosphate (RuBP) regeneration enzymes like FbaA might be a better choice for increasing CO_2 fixation. Two of the lower glycolysis enzymes that pull flux towards pyruvate, Pgm and Eno, also increased isoprene production. A previous study showed that overexpressing the lower glycolysis enzymes enhanced not only the production of the pyruvate derived product 2,3-butanediol, but also led to an increased carbon fixation in *S. elongatus* (Oliver and Atsumi, 2015). The same positive effect on carbon fixation was seen when sugars were being continuously removed from the metabolism (Ducat et al., 2012), indicating that creating a pull from the CBB cycle can be just as effective, or more, for increasing CO_2 fixation as is overexpressing the enzymes within the cycle.

Although overexpressing several genes from the general metabolism increased isoprene production, it is not certain that they did so by redirecting the flux through the MEP pathway or if it was a secondary effect, such as alleviating a metabolic imbalance or restoring a critical cellular component like amino acids depleted from the protein overexpression. An important example to keep in mind is the findings of several genes that when expressed in *E. coli* increased lycopene production (Alper et al., 2005; Wang et al., 2009). It was later discovered that due to the use of colorimetric assays in those studies and due to

lycopene degrading and turning colorless by reactive oxygen species, the mechanisms why some of those genes increased detected amounts of lycopene was likely not by directly affecting carbon flux towards terpenoids but instead by reducing cellular stress (Bongers et al., 2015).

A genome scale metabolic model was used to identify how the metabolic network needed to be remodeled to support an increase in isoprene production. Our modeling suggested an up-regulation of the CBB cycle and lower glycolysis to pyruvate. Furthermore, reactions involved in the supply and recycling of cofactors used in the MEP pathway, such as NADPH and CTP, were also to be up-regulated. The TCA cycle was identified as a carbon sink and required to be down-regulated. In comparison, *in silico* studies in *E. coli* suggested an up-regulation of the TCA cycle instead to support lycopene production (Choi et al., 2010). These opposite results are due the different natures of the autotrophic and heterotrophic metabolisms. In *E. coli*, the TCA cycle is required to provide reductants and ATP to support the flux going to the MEP pathway. In *Synechocystis* however, NADPH and ATP is readily provided by the light reactions. Therefore there is no need to up-regulate the TCA cycle. Interestingly, ATP synthase was suggested to be down-regulated. An *in silico* study showed that limonene production in *Synechocystis* could be increased by decreasing the ATP/NADPH ratio, thus creating an imbalance forcing product synthesis (Shabestary and Hudson, 2016). While we did not experimentally test this here, it is an interesting suggestion for future studies.

The FVSEOF method was performed by gradually increasing the flux going towards isoprene in the model and analyzing the changes in the metabolism. However, to get a significant change between the different flux states tested using the model, we set the isoprene values between 0 and 0.5 mmol/gCDW/h while our actual measured amount from the *SkIspS* strain was several orders of magnitude lower (0.04 μmol/gCDW/h). Despite these differences, implementing the results from FVSEOF could successfully improve isoprene titers, suggesting that overexpression of the identified targets could push the carbon flux towards isoprene synthesis. The model also identified the importance of cofactor availability and recycling, which we experimentally verified in the CTPs and ferredoxin expressing strains. When fluxes are further increased to approach theoretical limits in future studies, for example with the use of more efficient isoprene synthases increasing the metabolic pull towards isoprene synthesis, proper balance and supply of cofactors will need serious consideration, for which this kind of model can provide guidance.

The IspS substrate DMAPP together with IPP is essential for building terpenoid compounds that play critical roles in cell wall and membrane biosynthesis, light harvesting pigments, and in the respiratory electron transport chain (Perez-Gil and Rodriguez-Concepcion, 2013). Expressing the more efficient IbIspS and EgIspS could deplete DMAPP to levels where the production of terpenoids critical for cell viability was severely affected. That could explain why our initial attempts at expressing IbIspS and EgIspS in *Synechocystis* were all unsuccessful and why additional expression of Dxs and Ipi was required to be get viable cells. Although doing the MEP and upstream assay with the more efficient IspSs might have been beneficial for evaluating the effects of overexpression of the target enzymes in a cell where a more significant flux is going towards isoprene production, our strategy of probing each MEP enzyme individually in a strain only expressing IspS would not have been possible since they required MEP enzymes to be already expressed.

Although the impact of changing IspS played the most critical role in increasing isoprene production, overexpressing enzymes from ten other reactions all increased isoprene production in this study. Thus, the concept that there is only one bottleneck at a given time and all other reactions in the pathway are operating at less than their capacity is not accurate. Rather, several reaction steps can contribute to create a metabolic push towards a product. The results from this study indicate that IspS pulling substrate to isoprene is more efficient than upstream pathways pushing towards it. Thus, the most effective initial strategy for pure production focused studies would likely be to find a highly efficient terminal enzyme and create a large pull towards the production by expressing the enzyme as much as the cells can handle. Additional reactions would be expressed to prevent toxic effects of metabolite depletion or when catalytic rates of the final enzyme start to become saturated. This strategy of focusing on the terminal enzyme has been used to great effects for lactate (Angermayr and Hellingwerf, 2013), ethanol (Gao et al., 2012) and β- phellandrene (Formighieri and Melis, 2014) production in *Synechocystis*.

Several studies have been made on metabolic engineering of cyanobacteria for isoprene production. From the first report in *Synechocystis* of 50 μg/g per dry cell weight (Lindberg et al., 2010), the current highest reported titer of 1.26 g/L was achieved in *S. elongatus* (Gao et al., 2016). This improvement in production was primarily achieved by substituting the less efficient IspS from *P. montana* for IspS from *E. globulus* which led to a sharp increase in production, and also by overexpressing Dxs, IspG and a IspS-Ipi fusion. In *Synechocystis*, the highest reported titer is 12.3 mg/g per dry cell weight, using the *P. Montana* IspS fused to the highly expressed cpcB gene and overexpressing Ipi from *Streptococcus pneumoniae* (Chaves and Melis, 2018). In this work, the highest producing strain made 2.8 mg/g isoprene per dry cell weight or 1.0 mg/L (see Supplementary Table 3 for the isoprene production of each strain using several different units for comparison). However, our goal in this study was to use isoprene as a reporter for MEP pathway flux to find overexpression targets in a systematic way, and the cultivation conditions used were non-ideal for high production. Since the cells were grown in closed tubes, carbon was supplied as HCO_3^- but the oxygen evolved from the cells created a pressure buildup that could negatively affect production. A better cultivation system would have continuous bubbling of air through the culture, thereby supplying CO_2 and removing excess isoprene and O_2, followed by recovery of the product in the off-gas. A cultivation system of continuous product removal and recovery has been used to reach titers of 60 g/L isoprene per culture volume in *E. coli* (Whited et al., 2010).

In conclusion, we demonstrated here a terpenoid flux assay, probing each gene in the MEP pathway and some pathways from the general metabolism, selected by metabolic modeling, for increases in isoprene production. Additional studies need to be done to understand the actual mechanisms behind the changes on flux we saw. Still, the findings from this work can help in the bioproduction of a range of terpenoid compounds such as pharmaceuticals, cosmetics, biofuels and chemical feedstocks.

Acknowledgements

This work was supported by the Swedish Energy Agency (grant no 38334-1) and Swedish Foundation for Strategic Research (RBP-14-0013). The *Synechocystis* IspS-expressing strain was a gift from Dr. Anastasios Melis, University of California, Berkeley, and the sequence of EgIspS was provided by the lab of Chen Yang, Chinese Academy of Sciences, Shanghai.

Conflict of interests

The authors declare that there are no conflicts of interest.

Appendix A. Supplementary material

Supplementary data associated with this article can be found in the online version at doi:10.1016/j.ymben.2018.07.004.

References

Ajikumar, P.K., Xiao, W.H., Tyo, K.E., Wang, Y., Simeon, F., Leonard, E., Mucha, O., Phon, T.H., Pfeifer, B., Stephanopoulos, G., 2010. Isoprenoid pathway optimization for Taxol precursor overproduction in *Escherichia coli*. Science 330, 70–74.

Albrecht, M., Misawa, N., Sandmann, G., 1999. Metabolic engineering of the terpenoid biosynthetic pathway of *Escherichia coli* for production of the carotenoids β-carotene and zeaxanthin. Biotechnol. Lett. 21, 791–795.
Alper, H., Miyaoku, K., Stephanopoulos, G., 2005. Construction of lycopene-overproducing *E. coli* strains by combining systematic and combinatorial gene knockout targets. Nat. Biotechnol. 23, 612–616.
Anderson, J.C., Dueber, J.E., Leguia, M., Wu, G.C., Goler, J.A., Arkin, A.P., Keasling, J.D., 2010. BglBricks: a flexible standard for biological part assembly. J. Biol. Eng. 4, 1.
Angermayr, S.A., Hellingwerf, K.J., 2013. On the use of metabolic control analysis in the optimization of cyanobacterial biosolar cell factories. J. Phys. Chem. B 117, 11169–11175.
Atsumi, S., Higashide, W., Liao, J.C., 2009. Direct photosynthetic recycling of carbon dioxide to isobutyraldehyde. Nat. Biotechnol. 27, 1177.
Banerjee, A., Wu, Y., Banerjee, R., Li, Y., Yan, H., Sharkey, T.D., 2013. Feedback inhibition of deoxy-D-xylulose-5-phosphate synthase regulates the methylerythritol 4-phosphate pathway. J. Biol. Chem. 288, 16926–16936.
Bentley, F.K., Melis, A., 2012. Diffusion-based process for carbon dioxide uptake and isoprene emission in gaseous/aqueous two-phase photobioreactors by photosynthetic microorganisms. Biotechnol. Bioeng. 109, 100–109.
Bentley, F.K., García-Cerdán, J.G., Chen, H.-C., Melis, A., 2013. Paradigm of monoterpene (β-phellandrene) hydrocarbons production via photosynthesis in cyanobacteria. BioEnergy Res. 6, 917–929.
Bentley, F.K., Zurbriggen, A., Melis, A., 2014. Heterologous expression of the mevalonic acid pathway in cyanobacteria enhances endogenous carbon partitioning to isoprene. Mol. Plant. 7, 71–86.
Bongers, M., Chrysanthopoulos, P.K., Behrendorff, J.B., Hodson, M.P., Vickers, C.E., Nielsen, L.K., 2015. Systems analysis of methylerythritol-phosphate pathway flux in *E. coli*: insights into the role of oxidative stress and the validity of lycopene as an isoprenoid reporter metabolite. Microb. Cell Factor. 14, 193.
Chang, W.C., Song, H., Liu, H.W., Liu, P., 2013. Current development in isoprenoid precursor biosynthesis and regulation. Curr. Opin. Chem. Biol. 17, 571–579.
Chaves, J.E., Melis, A., 2018. Biotechnology of cyanobacterial isoprene production. Appl. Microbiol. Biotechnol. 1–8.
Chaves, J.E., Romero, P.R., Kirst, H., Melis, A., 2016. Role of isopentenyl-diphosphate isomerase in heterologous cyanobacterial (*Synechocystis*) isoprene production. Photosynth. Res. 130, 517–527.
Choi, H.S., Lee, S.Y., Kim, T.Y., Woo, H.M., 2010. In silico identification of gene amplification targets for improvement of lycopene production. Appl. Environ. Microbiol. 76, 3097–3105.
Choi, S.Y., Lee, H.J., Choi, J., Kim, J., Sim, S.J., Um, Y., Kim, Y., Lee, T.S., Keasling, J.D., Woo, H.M., 2016. Photosynthetic conversion of CO_2 to farnesyl diphosphate-derived phytochemicals (amorpha-4,11-diene and squalene) by engineered cyanobacteria. Biotechnol. Biofuels 9, 202.
Davies, F.K., Work, V.H., Beliaev, A.S., Posewitz, M.C., 2014. Engineering limonene and bisabolene production in wild type and a glycogen-deficient mutant of *Synechococcus* sp. PCC 7002. Front. Bioeng. Biotechnol. 2, 21.
Davies, F.K., Jinkerson, R.E., Posewitz, M.C., 2015. Toward a photosynthetic microbial platform for terpenoid engineering. Photosynth. Res. 123, 265–284.
Ducat, D.C., Avelar-Rivas, J.A., Way, J.C., Silver, P.A., 2012. Rerouting carbon flux to enhance photosynthetic productivity. Appl. Environ. Microbiol. 78, 2660–2668.
Eisenreich, W., Bacher, A., Arigoni, D., Rohdich, F., 2004. Biosynthesis of isoprenoids via the non-mevalonate pathway. Cell. Mol. Life Life Sci. CMLS 61, 1401–1426.
Elhai, J., Wolk, C.P., 1988. Conjugal transfer of DNA to cyanobacteria. Methods Enzymol. 167, 747–754.
Englund, E., Pattanaik, B., Ubhayasekera, S.J., Stensjo, K., Bergquist, J., Lindberg, P., 2014. Production of squalene in *Synechocystis* sp. PCC 6803. PLoS One 9, e90270.
Englund, E., Andersen-Ranberg, J., Miao, R., Hamberger, B.r., Lindberg, P., 2015. Metabolic engineering of *Synechocystis* sp. PCC 6803 for production of the plant diterpenoid manoyl oxide. ACS Synth. Biol. 4, 1270–1278.
Formighieri, C., Melis, A., 2014. Regulation of β-phellandrene synthase gene expression, recombinant protein accumulation, and monoterpene hydrocarbons production in *Synechocystis* transformants. Planta 240, 309–324.
Formighieri, C., Melis, A., 2015. A phycocyanin.phellandrene synthase fusion enhances recombinant protein expression and beta-phellandrene (monoterpene) hydrocarbons production in *Synechocystis* (cyanobacteria). Metab. Eng. 32, 116–124.
Gao, X., Gao, F., Liu, D., Zhang, H., Nie, X., Yang, C., 2016. Engineering the methylerythritol phosphate pathway in cyanobacteria for photosynthetic isoprene production from CO_2. Energy Environ. Sci. 9, 1400–1411.
Gao, Z., Zhao, H., Li, Z., Tan, X., Lu, X., 2012. Photosynthetic production of ethanol from carbon dioxide in genetically engineered cyanobacteria. Energy Environ. Sci. 5, 9857–9865.
Gruchattka, E., Hadicke, O., Klamt, S., Schutz, V., Kayser, O., 2013. In silico profiling of *Escherichia coli* and *Saccharomyces cerevisiae* as terpenoid factories. Microb. Cell Factor. 12, 84.
Halfmann, C., Gu, L., Zhou, R., 2014. Engineering cyanobacteria for the production of a cyclic hydrocarbon fuel from CO_2 and H_2O. Green Chem. 16, 3175–3185.
Huang, H.-H., Camsund, D., Lindblad, P., Heidorn, T., 2010. Design and characterization of molecular tools for a Synthetic Biology approach towards developing cyanobacterial biotechnology. Nucleic Acids Res. 38, 2577–2593.
Ilmén, M., Oja, M., Huuskonen, A., Lee, S., Ruohonen, L., Jung, S., 2015. Identification of novel isoprene synthases through genome mining and expression in *Escherichia coli*. Metab. Eng. 31, 153–162.
Ivleva, N.B., Golden, S.S., 2007. Protein extraction, fractionation, and purification from cyanobacteria. Methods Mol. Biol. 362, 365–373.
Kiyota, H., Okuda, Y., Ito, M., Hirai, M.Y., Ikeuchi, M., 2014. Engineering of cyanobacteria for the photosynthetic production of limonene from CO_2. J. Biotechnol. 185, 1–7.
Kosuri, S., Goodman, D.B., Cambray, G., Mutalik, V.K., Gao, Y., Arkin, A.P., Endy, D., Church, G.M., 2013. Composability of regulatory sequences controlling transcription and translation in *Escherichia coli*. Proc. Natl. Acad. Sci. USA 110, 14024–14029.
Kudla, G., Murray, A.W., Tollervey, D., Plotkin, J.B., 2009. Coding-sequence determinants of gene expression in *Escherichia coli*. Science 324, 255–258.
Kudoh, K., Hotta, S., Sekine, M., Fujii, R., Uchida, A., Kubota, G., Kawano, Y., Ihara, M., 2017. Overexpression of endogenous 1-deoxy-D-xylulose 5-phosphate synthase (DXS) in cyanobacterium *Synechocystis* sp. PCC6803 accelerates protein aggregation. J. Biosci. Bioeng. 123, 590–596.
Leavell, M.D., McPhee, D.J., Paddon, C.J., 2016. Developing fermentative terpenoid production for commercial usage. Curr. Opin. Biotechnol. 37, 114–119.
Lee, J.-K., Oh, D.-K., Kim, S.-Y., 2007. Cloning and characterization of the dxs gene, encoding 1-deoxy-D-xylulose 5-phosphate synthase from *Agrobacterium tumefaciens*, and its overexpression in *Agrobacterium tumefaciens*. J. Biotechnol. 128, 555–566.
Liang, F., Lindblad, P., 2016. Effects of overexpressing photosynthetic carbon flux control enzymes in the cyanobacterium *Synechocystis* PCC 6803. Metab. Eng. 38, 56–64.
Liang, F., Lindblad, P., 2017. Synechocystis PCC 6803 overexpressing RuBisCO grow faster with increased photosynthesis. Metab. Eng. Commun. 4, 29–36.
Liang, F., Englund, E., Lindberg, P., Lindblad, P., 2018. Engineered cyanobacteria with enhanced growth show increased ethanol production and higher biofuel to biomass ratio. Metab. Eng.
Lindberg, P., Park, S., Melis, A., 2010. Engineering a platform for photosynthetic isoprene production in cyanobacteria, using *Synechocystis* as the model organism. Metab. Eng. 12, 70–79.
Lou, C., Stanton, B., Chen, Y.J., Munsky, B., Voigt, C.A., 2012. Ribozyme-based insulator parts buffer synthetic circuits from genetic context. Nat. Biotechnol. 30, 1137–1142.
Lv, X., Gu, J., Wang, F., Xie, W., Liu, M., Ye, L., Yu, H., 2016. Combinatorial pathway optimization in *Escherichia coli* by directed co-evolution of rate-limiting enzymes and modular pathway engineering. Biotechnol. Bioeng. 113, 2661–2669.
Martin, V.J., Pitera, D.J., Withers, S.T., Newman, J.D., Keasling, J.D., 2003. Engineering a mevalonate pathway in *Escherichia coli* for production of terpenoids. Nat. Biotechnol. 21, 796–802.
Matsushima, D., Jenke-Kodama, H., Sato, Y., Fukunaga, Y., Sumimoto, K., Kuzuyama, T., Matsunaga, S., Okada, S., 2012. The single cellular green microalga *Botryococcus braunii*, race B possesses three distinct 1-deoxy-D-xylulose 5-phosphate synthases. Plant Sci. 185, 309–320.
Mutalik, V.K., Guimaraes, J.C., Cambray, G., Lam, C., Christoffersen, M.J., Mai, Q.A., Tran, A.B., Paull, M., Keasling, J.D., Arkin, A.P., Endy, D., 2013a. Precise and reliable gene expression via standard transcription and translation initiation elements. Nat. Methods 10, 354–360.
Mutalik, V.K., Guimaraes, J.C., Cambray, G., Mai, Q.A., Christoffersen, M.J., Martin, L., Yu, A., Lam, C., Rodriguez, C., Bennett, G., Keasling, J.D., Endy, D., Arkin, A.P., 2013b. Quantitative estimation of activity and quality for collections of functional genetic elements. Nat. Methods 10, 347–353.
Nogales, J., Gudmundsson, S., Knight, E.M., Palsson, B.O., Thiele, I., 2012. Detailing the optimality of photosynthesis in cyanobacteria through systems biology analysis. Proc. Natl. Acad. Sci. 109, 2678–2683.
Okada, K., Hase, T., 2005. Cyanobacterial non-mevalonate pathway (E)-4-hydroxy-3-methylbut-2-enyl diphosphate synthase interacts with ferredoxin in *Thermosynechococcus elongatus* BP-1. J. Biol. Chem. 280, 20672–20679.
Oliver, J.W., Atsumi, S., 2015. A carbon sink pathway increases carbon productivity in cyanobacteria. Metab. Eng. 29, 106–112.
Pade, N., Erdmann, S., Enke, H., Dethloff, F., Duhring, U., Georg, J., Wambutt, J., Kopka, J., Hess, W.R., Zimmermann, R., Kramer, D., Hagemann, M., 2016. Insights into isoprene production using the cyanobacterium *Synechocystis* sp. PCC 6803. Biotechnol. Biofuels 9, 89.
Park, J.M., Park, H.M., Kim, W.J., Kim, H.U., Kim, T.Y., Lee, S.Y., 2012. Flux variability scanning based on enforced objective flux for identifying gene amplification targets. BMC Syst. Biol. 6, 106.
Perez-Gil, J., Rodriguez-Concepcion, M., 2013. Metabolic plasticity for isoprenoid biosynthesis in bacteria. Biochem. J. 452, 19–25.
Poncelet, M., Cassier-Chauvat, C., Leschelle, X., Bottin, H., Chauvat, F., 1998. Targeted deletion and mutational analysis of the essential (2Fe–2S) plant-like ferredoxin in *Synechocystis* PCC6803 by plasmid shuffling. Mol. Microbiol. 28, 813–821.
Puan, K.-J., Wang, H., Dairi, T., Kuzuyama, T., Morita, C.T., 2005. fldA is an essential gene required in the 2-C-methyl-D-erythritol 4-phosphate pathway for isoprenoid biosynthesis. FEBS Lett. 579, 3802–3806.
Qi, L., Haurwitz, R.E., Shao, W., Doudna, J.A., Arkin, A.P., 2012. RNA processing enables predictable programming of gene expression. Nat. Biotechnol. 30, 1002–1006.
Ranganathan, S., Suthers, P.F., Maranas, C.D., 2010. OptForce: an optimization procedure for identifying all genetic manipulations leading to targeted overproductions. PLoS Comput. Biol. 6, e1000744.
Salis, H.M., Mirsky, E.A., Voigt, C.A., 2009. Automated design of synthetic ribosome binding sites to control protein expression. Nat. Biotechnol. 27, 946–950.
Schellenberger, J., Que, R., Fleming, R.M., Thiele, I., Orth, J.D., Feist, A.M., Zielinski, D.C., Bordbar, A., Lewis, N.E., Rahmanian, S., 2011. Quantitative prediction of cellular metabolism with constraint-based models: the COBRA Toolboxv2. 0. Nat. Protoc. 6, 1290.
Shabestary, K., Hudson, E.P., 2016. Computational metabolic engineering strategies for growth-coupled biofuel production by *Synechocystis*. Metab. Eng. Commun. 3, 216–226.
Shen, C.R., Lan, E.I., Dekishima, Y., Baez, A., Cho, K.M., Liao, J.C., 2011. Driving forces enable high-titer anaerobic 1-butanol synthesis in *Escherichia coli*. Appl. Environ. Microbiol. 77, 2905–2915.
Wang, H.H., Isaacs, F.J., Carr, P.A., Sun, Z.Z., Xu, G., Forest, C.R., Church, G.M., 2009.

Programming cells by multiplex genome engineering and accelerated evolution. Nature 460, 894–898.
White, J.K., Handa, S., Vankayala, S.L., Merkler, D.J., Woodcock, H.L., 2016. Thiamin diphosphate activation in 1-deoxy-D-xylulose 5-phosphate synthase: insights into the mechanism and underlying intermolecular interactions. J. Phys. Chem. B 120, 9922–9934.
Whited, G.M., Feher, F.J., Benko, D.A., Cervin, M.A., Chotani, G.K., McAuliffe, J.C., LaDuca, R.J., Ben-Shoshan, E.A., Sanford, K.J., 2010. Technology update: development of a gas-phase bioprocess for isoprene-monomer production using metabolic pathway engineering. Ind. Biotechnol. 6, 152–163.
Xiang, S., Usunow, G., Lange, G., Busch, M., Tong, L., 2012. 1-Deoxy-d-Xylulose 5-Phosphate Synthase (DXS), a crucial enzyme for isoprenoids biosynthesis. In: Bach, Thomas J., Rohmer, Michel (Eds.), Isoprenoid Synthesis in Plants and Microorganisms. Springer, New York, pp. 17–28.
Ye, L., Lv, X., Yu, H., 2016. Engineering microbes for isoprene production. Metab. Eng. 38, 125–138.
Zhou, J., Yang, L., Wang, C., Choi, E.-S., Kim, S.-W., 2017. Enhanced performance of the methylerythritol phosphate pathway by manipulation of redox reactions relevant to IspC, IspG, and IspH. J. Biotechnol. 248, 1–8.
Zhou, K., Zou, R., Stephanopoulos, G., Too, H.-P., 2012. Enhancing solubility of deoxyxylulose phosphate pathway enzymes for microbial isoprenoid production. Microb. Cell Factor. 11, 148.
Zurbriggen, A., Kirst, H., Melis, A., 2012. Isoprene production via the mevalonic acid pathway in *Escherichia coli* (bacteria). BioEnergy Res. 5, 814–828.